Environmental Science
Processes & Impacts

PAPER

View Article Online
View Journal | View Issue

Cite this: *Environ. Sci.: Processes Impacts*, 2019, **21**, 1722

Biochar particle aggregation in soil pore water: the influence of ionic strength and interactions with pyrene†

Stephanie Castan, [a] Gabriel Sigmund, [abc] Thorsten Hüffer [a] and Thilo Hofmann *[a]

Received 6th June 2019
Accepted 31st July 2019

DOI: 10.1039/c9em00277d

rsc.li/espi

The beneficial properties of biochar have led to its increasing application to soils for environmental management. Despite its stability in soil, biochar can physically disintegrate into smaller particles, which can then be relocated from the application area. Biochar transport is strongly dependent on the biochar particle size and aggregation, with the extent of aggregation depending on the chemistry of the soil pore water. Biochar has a strong sorption affinity for polyaromatic hydrocarbons (PAHs) such as pyrene, which can also affect its transport. We therefore investigated biochar particle aggregation in solutions of different ionic strengths (ultrapure water, 0.01 M $CaCl_2$, and 0.1 M $CaCl_2$) with suspensions of biochar particles, and with suspensions of biochar particles loaded with pyrene (0.2 and 3.6 g kg^{-1}). Increasing the pyrene concentration in ultrapure water resulted in an increase in the biochar particle size, an effect that was more pronounced following equilibration for 28 days than following equilibration for only 24 hours. Biochar particle aggregation in solutions containing both pyrene and 0.01 M $CaCl_2$ was greatly enhanced compared to aggregation in similar solutions with no pyrene. However, the influence of pyrene became negligible at high $CaCl_2$ concentrations (0.1 M $CaCl_2$). To determine the fate of biochar in soil, both the presence of PAHs and the influence of the pore water's ionic strength therefore need to be taken into account.

Environmental significance

Biochar is increasingly being used for environmental management including soil improvement, contaminant remediation, and carbon sequestration, and has potential for large scale applications. Although it is chemically stable over long periods of time, biochar can physically disintegrate and be relocated as fines. Biochar particle transport is expected to be largely dependent on the sizes of the particles and their aggregates, the latter depending in turn on the solution chemistry. We investigated the influence of ionic strength and pyrene (a ubiquitous representative of polyaromatic hydrocarbons) on biochar aggregation. The results of these investigations contribute to an improved mechanistic understanding of the factors influencing the aggregation and transport of biochar particles in soil.

1. Introduction

Biochar is produced by the pyrolysis of biomass such as wood, agricultural residues, or animal and municipal waste at temperatures ranging from 350 °C to 1000 °C, under limited oxygen supply.[1] The resulting amorphous carbonaceous material is composed of randomly stacked flat aromatic (carbon-based) sheets with oxygen-containing functional groups such as carboxylic, phenolic, hydroxyl, carbonyl, and quinone groups on their edges.[2] With increasing pyrolysis temperature the amorphous aromatic sheets become more aligned until reaching an almost graphitic structure at very high temperatures.[3] The properties of biochar, such as its long term stability in soil resulting from its high degree of carbonization, high specific surface area, porosity, and hydrophobicity, have led to its increasing use in environmental management, for example for carbon sequestration in soils,[4] for nutrient retention,[5] and for remediation of organic pollutants, for example polyaromatic hydrocarbons (PAHs).[6]

Although considered recalcitrant, biochar can be subject to considerable physical disintegration and subsequent transport through soil,[7–9] with biochar particle transport increasing as the particle size decreases.[10–12] However, biochar transport is influenced not only by its disintegration, but it is also strongly

[a]Department of Environmental Geosciences, Centre for Microbiology and Environmental Systems Science, University of Vienna, Althanstraße 14, 1090 Wien, Austria. E-mail: thilo.hofmann@univie.ac.at; Tel: +43-1-4277-53320
[b]Agroscope, Environmental Analytics, Reckenholzstrasse 191, CH-8046 Zurich, Switzerland
[c]Ithaka Institute for Carbon Strategies, Ancienne Eglise 9, Arbaz 1974, Switzerland

† Electronic supplementary information (ESI) available. See DOI: 10.1039/c9em00277d

affected by particle aggregation which depends on the pore water chemistry.[13–15]

Biochar particle aggregation generally follows Derjaguin–Landau–Verwey–Overbeek (DLVO) theory, which explains aggregation as a function of van der Waals attraction and electrostatic repulsion,[16,17] with the latter having a positive correlation with the degree of oxidation on the biochar surfaces and the functional groups present.[18–21] The presence of divalent Ca^{2+} ions has been shown to enhance aggregation through double layer compression and cation bridging.[11,19] According to the Schulze–Hardy rule, the aggregation power of a counterion is strongly dependent on its valence.[20,21] Monovalent ions such as Na^{+} therefore only induce particle aggregation when present at much higher concentrations than more highly charged cations.[9]

Biochar has slow rates of downward migration within the soil,[7] providing the time for equilibration with the surrounding pore water, which can affect the aggregation of biochar particles. Laboratory scale experiments therefore need to take into account the equilibration times of all processes that might influence the experimental results. This includes water uptake by biochar, which is dependent on porosity and hydrophobicity and can take more than 21 days.[22] The adsorption of PAHs such as naphthalene or pyrene is also limited kinetically.[23,24]

Biochar can be applied to soils to remediate and immobilize PAHs. The high sorption affinity of biochar for PAHs such as pyrene[6,25] can reduce the bioavailability of the PAH on-site and reduce its transport off-site.[26] Biochar can bind organic contaminants by two orders of magnitude more effectively than amorphous organic matter present in soil; it thereby can control both the contaminants' ecotoxicology and fate in soil.[27] But also the fate of biochar can be affected by the adsorbed PAHs with possible unknown effects on further transport of the biochar-bound PAH. The presence of PAHs has been found to enhance biochar retention in soils, which has been attributed to charge-shielding by the adsorbed PAHs, facilitating biochar–soil interactions.[9] However, the effects of ionic strength (IS) and sorbed PAHs on biochar particle transport have, to date, only been investigated separately and not in combination.

The aim of this study is to investigate biochar particle stability in relation to soil pore water chemistry and the presence of a model PAH, pyrene. We set out to test the hypothesis that IS and adsorbed PAHs have an interdependent influence on the aggregation of biochar.

2. Materials and methods

The biochar used (SWP700) was a UKBRC (UK Biochar Research Center) standard biochar produced from softwood pellets at a pyrolysis temperature of 700 °C. Prior to experimentation the biochar was crushed and sieved to obtain <250 μm size fraction. All chemicals used were of analytical grade, including pyrene (Sigma Aldrich, Germany, Table S1†), pyrene-d10 (Dr Ehrenstorfer GmbH, Germany), $CaCl_2$ (Merck, Germany), hexane (>99% purity, VWR, Germany), methanol, (>99.5% purity, VWR, Germany) and NaN_3 (99%, extra pure, ACROS Organics, Belgium).

2.1. Aggregation experiments

Triplicates of biochar suspensions (250 mg L^{-1}) were prepared according to a similar ratio as used in a previous study (200 mg L^{-1})[11] either in ultrapure water (MQ, Millipore, Elix®5-Milli-Q® Gradient A10, SI2, Germany), in 0.01 M $CaCl_2$ or in 0.1 M $CaCl_2$ solutions. The samples were shaken at 125 rpm for either 24 hours or 28 days. The 0.01 M $CaCl_2$ solution was used to represent soil pore water IS according to OECD guideline 106,[28] and the 0.1 M $CaCl_2$ solution was used for mechanistic comparisons, exceeding the critical coagulation concentration of $CaCl_2$ previously determined for wheat straw and pinewood biochar pyrolyzed at 600 °C (0.038 M and 0.042 M, respectively)[29,30] and for wood shaving biochar pyrolyzed at 400 °C (0.075 M).[31] Pyrene (stock solution in MeOH) was spiked to initial aqueous concentrations of 100 μg L^{-1} and 1500 μg L^{-1}. The volume spiked was kept below 0.25% of the total volume to avoid co-solvent effects. Following equilibration, the pH was recorded and particle size distributions were measured on the basis of the time-of-transition principle, using an EyeTech particle size analyzer (laser shading, Ankersmid Laboratory, the Netherlands). The measurement range of the laser lens (A100) was 0.6–300 μm and three 60 second measurements were carried out for each sample. D50 values of the number-based size distributions (*i.e.* the particle size at which 50% of the measured particles were smaller) were used in the data analysis. The electrophoretic mobility of the particles was measured (using a ZetaSizer Nano ZS, Malvern Instruments Ltd., UK) in order to then calculate their ζ-potential using the Smoluchowski equation. For each of the samples, three sets of measurements, each comprising 20 runs, were stacked; the conductivity was > 2 μS cm^{-1} in MQ water, >2 mS cm^{-1} in the 0.01 M $CaCl_2$ solution, and >16 mS cm^{-1} in the 0.1 M $CaCl_2$ solution. The averaged measurements from the three sets of sample runs were used in data interpretation. The total CHNS content was determined using an elemental analyzer (Vario MACRO, Elementar, Germany) and the average of 5 individual measurements was recorded. The oxygen content was estimated by mass balance: O% = 100 − (C + H + N + S + ash content).

2.2. Sorption experiments

The sorption of pyrene to biochar after 28 days was determined in separate experiments using polyoxymethylene (POM) sheets as passive samplers, adapting a protocol previously described by Kah *et al.*[32] The use of POM sheets allows significantly lower sorbate concentrations to be determined than is possible using classical two-phase batch-equilibrium methods. The POM sheets (each with 1 cm^2 squares, a thickness of 0.5 mm, and a density 1.4 g cm^{-2}) were cold extracted by shaking with hexane and methanol. Suspensions of biochar (10 ± 1 mg) in 40 mL MQ water or 0.01 M $CaCl_2$ background solution, each containing 25 mg L^{-1} NaN_3 as the bioinhibitor, were prepared in 50 mL glass vials with Teflon screw caps. One POM sheet was added to each sample. Pyrene (stock solution in MeOH) was spiked to initial aqueous concentrations ranging from 0.25 to 125 μg L^{-1}, including two duplicate samples. The volume spiked was kept below 0.3% of the total volume to avoid co-solvent effects. After

spiking, the samples were agitated at 125 rpm for 28 days under the exclusion of light. The POM sheets were then removed from the vials, carefully wiped with a lint-free tissue to remove any sorbent remaining on the surface, and spiked with an internal standard (0.25 μg of d10-pyrene from a methanolic stock solution). Following cold extraction over 3 days with hexane, the solutions were concentrated for GC-MS analysis to approximately 1 mL, under a N_2 gas flow at 50 °C.

Since the POM method was not suitable for measuring the sorption after 24 hours a classical two-phase batch-equilibrium method was used according to OECD Guideline 106.[28] It has previously been demonstrated that batch and POM methods can be used as complementary methods.[32,33] The samples were equilibrated for 24 hours following a similar sample preparation to that described above but without adding any POM sheets, then centrifuged at 1000 g for 40 minutes and 30 mL of the supernatant was collected, which was then extracted three times with hexane following the addition of the internal standard (Pyr-d10).

Pyrene was quantified using gas chromatography mass spectrometry (GC-MS, Agilent Technologies, Germany; GC 7890A coupled to a 5975C inert XL MSD; 60 m HP-5MS capillary column, J&W Scientific). Helium was used as a carrier gas, with a flow rate of 1 mL min^{-1}. The initial oven temperature was 55 °C; it was then ramped to 300 °C at a rate of 20 °C min^{-1}. The limit of detection was determined as three times the signal to noise ratio for 9 blank measurements and yielded 5.4 ng L^{-1} for the batch sorption experiments and 0.2 ng L^{-1} for the POM passive sampling. Sorption isotherms are presented in the ESI† and sorption coefficients (K_D, L kg^{-1}) were compared at aqueous pyrene concentrations of 0.1, 1 and 10 μg L^{-1}.

3. Results and discussion

3.1. Increased biochar aggregation after longer equilibration time

The D50 value of the biochar particle size distribution in each solution after 24 hours was compared with that after 28 days (Fig. 1). Pyrene was found not to have had any influence on the biochar particle size after 24 hours in MQ water (1.15 ± 0.07 μm), but after 28 days the particle size was found to have increased slightly (from 1.41 ± 0.0 μm to 1.68 μm ± 0.45). Although the size differences were not statistically significant due to the standard deviation of the measurements, there did appear to be an increasing trend. A larger difference between 24 hours and 28 days was observed in the 0.01 M $CaCl_2$ solution. In this case the size of biochar particles increased from 1.52 ± 0.08 μm after 24 hours to 2.14 ± 0.15 μm after 28 days without any pyrene. In the presence of pyrene, aggregation was statistically significantly higher after 28 days than after 24 hours ($p < 0.05$) for all pyrene concentrations tested.

There was no difference between the adsorption of pyrene in MQ water and that in 0.01 M $CaCl_2$ solution (Fig. S1†), as would be expected for a non-polar compound.[26] However, a comparison of K_D values in 0.01 M $CaCl_2$ after 24 hours and 28 days at aqueous pyrene concentrations of 0.1, 1 and 10 μg L^{-1} (Fig. 2) showed that there was significantly less adsorption after 24

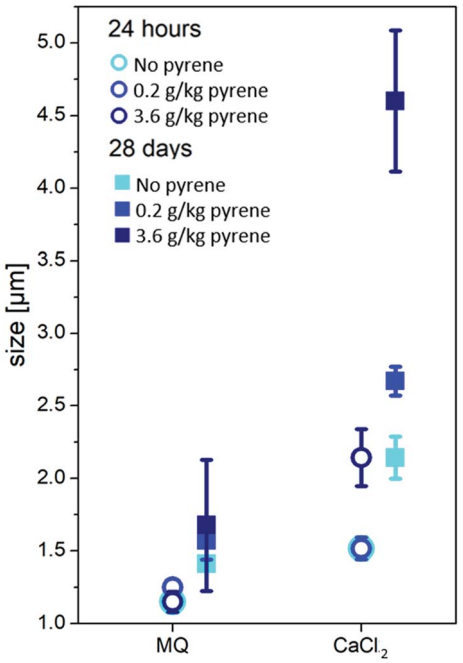

Fig. 1 Biochar particle size (D50) after 24 hours (○) and 28 days (■), in MQ water and 0.01 M $CaCl_2$ at different pyrene concentrations. In solutions with high ionic strengths and pyrene, there was significantly less aggregation after 24 hours than after 28 days.

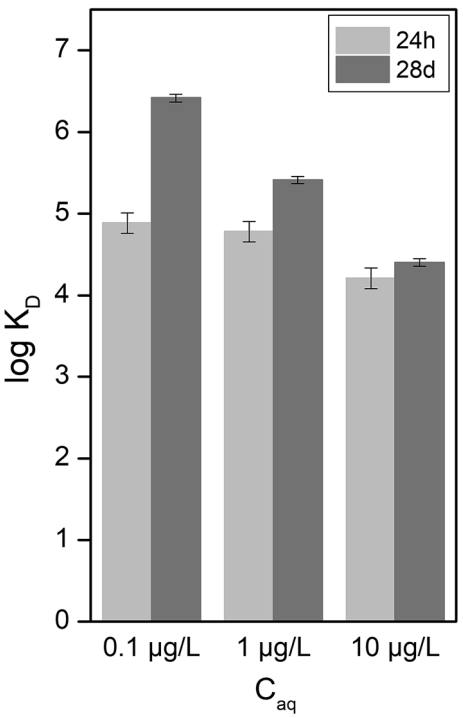

Fig. 2 Comparison of log K_D values for pyrene adsorption to biochar in 0.01 M $CaCl_2$ at aqueous pyrene concentrations of 0.1, 1 and 10 μg L^{-1}. Adsorption was significantly less after 24 hours of equilibration than after 28 days.

hours than after 28 days, which is in agreement with the results from previous sorption kinetic investigations.[23,24] This is in good agreement with the increase in biochar aggregation with increased pyrene sorption after 28 days (Fig. 1). These results show that the effects on biochar aggregation, which are barely observable over typically used time scales in laboratory experiments (<24 hours),[29,34,35] are more pronounced over extended periods of time.

3.2. Biochar aggregation enhanced by pyrene adsorption at low ionic strengths

The effect of pyrene on the biochar particle size after 28 days in MQ water was compared with that in the 0.01 M $CaCl_2$ background solution. Biochar aggregation was also tested under the influence of the high IS of a 0.1 M $CaCl_2$ solution in selected samples (Fig. 3). Increasing the pyrene concentration in MQ water yielded a less negative ζ-potential, resulting in increased particle aggregation and a slight increase in the measured biochar particle size, which is especially apparent in the size range between 20 and 40 μm (Fig. 4). The sorption of PAHs to biochar is generally controlled by a combination of hydrophobic partitioning into the non-carbonized phase of the biochar and adsorption of the carbonized phase of the biochar through π–π interactions with aromatic surfaces, which can be further influenced by pore-filling mechanisms.[36] The relative proportions contributed by the different interactions depend on the biochar feedstock and pyrolysis temperature.[36,37] The adsorption of PAHs to biochar charred at 700 °C was found to be almost exclusively driven by the adsorption to aromatic sites on the biochar surfaces, as a result of the high degree of carbonization and aromaticity of the biochar.[38] This adsorption mechanism is likely also the most dominant for the biochar used, as was confirmed by its elemental composition: the low H/C and O/C ratios (0.184 and 0.04, respectively) indicate a high degree of carbonization and aromaticity.

However, the high concentration of pyrene on the biochar surfaces (loading of 0.2 and 3.6 g kg^{-1}) can lead to additional attachment to less favorable sorption sites, such as surface functional groups, through n–π interactions and H-bonds.[24,39] It has previously been shown that weak n–π interactions can occur between PAHs such as pyrene (π-electron acceptor) and oxygen-containing functional groups (n-electron donors) of graphene oxides, especially carboxyl groups.[40] Furthermore, strong adsorption energies were calculated (using a density function theory model) for hydrogen bonds between pyrene and both the carboxyl groups and the hydroxyl groups on the biochar basal plane.[24] The less negative ζ-potential in the presence of pyrene (Fig. 3b) can therefore be explained as being due to H-bonds and n–π interactions between the pyrene and carboxyl or hydroxyl groups on the biochar surfaces.

A similar effect was observed by Yang *et al.*,[9] who noted a less negative biochar ζ-potential when naphthalene was present in a NaCl background electrolyte solution. Although this did not induce particle aggregation, it did enhance biochar retention in soil column experiments (*i.e.* the interactions of biochar with soil minerals), which they attributed to the charge-shielding effect of the adsorbed PAHs reducing the electrostatic repulsion by soil minerals. The greater influence of pyrene on the biochar particle size observed in this study may have been due to the long equilibration times and higher concentrations used, with the lowest pyrene concentration in this study corresponding to the highest naphthalene concentration used by Yang *et al.*[9]

As expected, increasing the $CaCl_2$ concentrations led to an increase in the biochar particle size due to an increase in aggregation, possibly due to both double layer compression and Ca^{2+} bridging resulting in a reduced ζ-potential (Fig. 3). Following the addition of pyrene to the 0.01 M $CaCl_2$ background solution, the combined effect of pyrene and the high IS resulted in a significantly stronger aggregation of biochar than that in background solutions with either pyrene and no $CaCl_2$, or 0.01 M $CaCl_2$ and no pyrene ($p < 0.05$). Improved suspension stability, even at elevated ionic strengths, has been linked to a high abundance of negative surface functional groups, which increase the electrostatic repulsion between particles.[41,42] However, the adsorption of pyrene may shield the surface charge, resulting in the reduction in both electrostatic repulsion and particle stability.

Furthermore, the much greater increase in particle size to 4.6 ± 0.49 μm after the addition of both 0.01 M $CaCl_2$ and pyrene

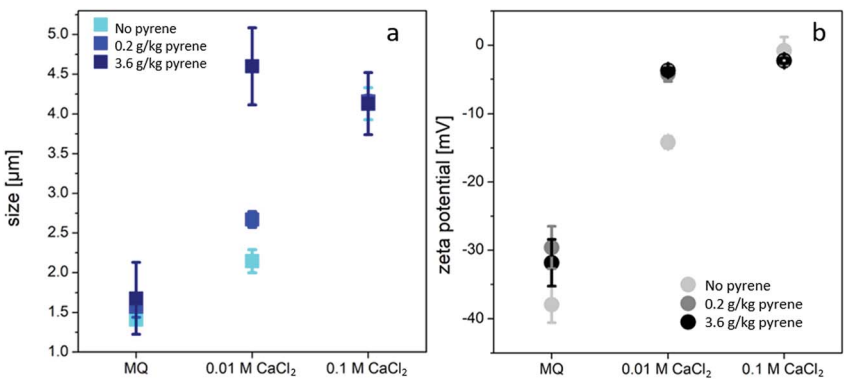

Fig. 3 (a) Size and (b) ζ-potential for biochar particles in different solutions after 28 days. Adsorbed pyrene enhanced aggregation at lower ionic strengths.

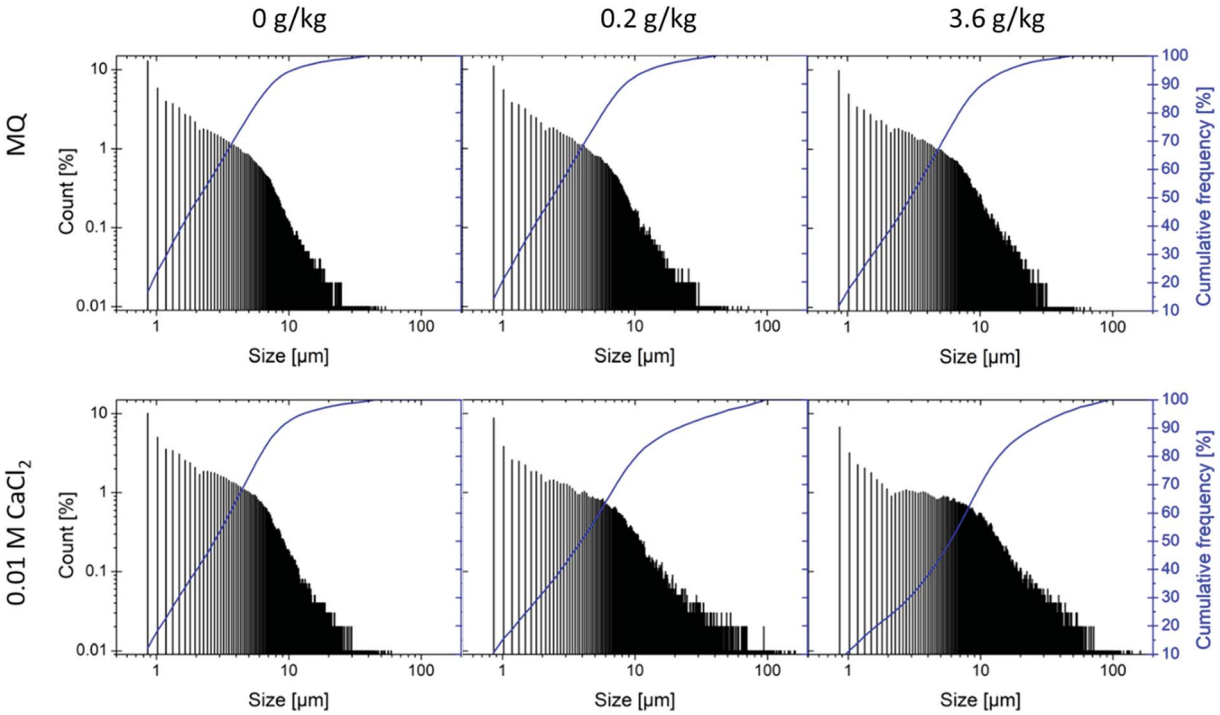

Fig. 4 Particle size distribution after 28 days in MQ water and in a 0.01 M $CaCl_2$ solution with biochar-pyrene loadings of 0, 0.2 and 3.6 g kg^{-1}.

together indicates a synergistic effect on biochar aggregation. This can be explained as being due to the formation of ternary cation–π–π complexes. Quiñonero *et al.*[43] showed that cation–π interactions and π–π interactions reinforce each other by forming strong ternary cation–π–π complexes. The interactions within these complexes are stronger than the sum of the two individual interactions. The presence of Ca^{2+} ions may therefore lead to a redistribution of pyrene π-electron densities. The enhanced electron-accepting properties of pyrene may then result in strong interactions between the pyrene and electron-donating sites on the biochar surfaces.[43,44]

In contrast, pyrene had no influence on biochar aggregation in solutions with 0.1 M $CaCl_2$. The critical coagulation concentration for $CaCl_2$ has previously been determined for wheat straw biochar pyrolyzed at 600 °C (0.038 M),[29] and for wood shaving biochar pyrolyzed at 400 °C (0.075 M).[31] In good agreement with this, pyrene aggregation could not be enhanced in the 0.1 M $CaCl_2$ solution, because the IS of 0.1 M $CaCl_2$ exceeds previously reported critical coagulation concentrations[29,30,35] so the maximum attachment efficiency of the biochar particles has already been reached. The enhanced aggregation induced by the adsorbed pyrene could only occur below those concentrations in 0.01 M $CaCl_2$ solutions at which charge neutralization by pyrene acts together with the double layer compression by Ca^{2+}. Biochar particles with adsorbed pyrene in a 0.01 M $CaCl_2$ background solution therefore formed aggregates that yielded similar particle sizes to biochar particles with no adsorbed pyrene in a 0.1 M $CaCl_2$ solution (Fig. 3a). Biochar particles in 0.1 M NaCl solution did not trigger any similar particle aggregation[9] due to the far less effective double layer compression by monovalent ions,[20,21] even with up to 100 µg L^{-1} naphthalene.

The particle size distributions showed high polydispersity, which increased with $CaCl_2$ and pyrene concentrations (Fig. 4). Although there was no apparent reduction in the number of the smallest particles (around 1 µm), the number of aggregates larger than 10 µm increased with increasing $CaCl_2$ and pyrene concentrations. This is in good agreement with previous findings showing that micro- and nanosized biochar particles (<1 µm and <0.1 µm, respectively) have a considerably higher content of oxygen-containing functional groups than larger biochar particles (<60 µm).[13] These can greatly enhance biochar particle stability and the count of particles with sizes around 1 µm consequently remained stable, while particles with sizes between 2 and 5 µm aggregated to sizes between 5 and 100 µm.

4. Conclusion

The transport and fate of biochar following its application to soils need to be fully understood before it can be used for large-scale soil amendment and environmental management. The processes influencing biochar aggregation have typically been investigated in the laboratory over only short periods of time (less than 24 hours).[29,31,34] We have shown, however, that the effects of pyrene and $CaCl_2$ on biochar aggregation are barely observable over such short time scales, whereas strong synergistic effects were observed after 28 days. Laboratory experiments investigating the processes that influence biochar aggregation, specifically the adsorption of PAHs or water uptake by biochar, therefore need to be carried out over extended periods of time.

The mobility of very fine biochar particles is expected to decrease in the presence of PAHs and at IS values commonly used in OECD guidelines for soil pore water, since such conditions tend to promote aggregation and attachment to soil. The adsorption of pyrene to biochar surfaces at low $CaCl_2$ concentrations was found to cause partial neutralization of the negative biochar surface charge and to enhance the aggregation of biochar particles. The interplay between charge neutralization by adsorbed pyrene and double layer compression by a $CaCl_2$ background electrolyte resulted in significantly stronger aggregation of biochar particles than that with pyrene but no $CaCl_2$, or with 0.01 M $CaCl_2$ and no pyrene. The fate of biochar fines in soil is therefore not determined solely by their physical disintegration, but is also strongly dependent on the chemical parameters of the soil pore water. Furthermore, our results show that the effects of the IS and the sorption of PAHs on biochar aggregation cannot be evaluated independently, since their effects on biochar stability are interdependent.

These findings improve the understanding of the fate of biochar in soil following its application and add to the knowledge base required for the use of biochar in large-scale soil amendments for environmental management.

Future investigations should include biochar with different surface functional properties. Biochar produced at lower pyrolysis temperatures, for example, as well as physically and chemically aged biochar contains more surface functional groups and is therefore expected to be more effective at stabilizing biochar in suspensions.

Conflicts of interest

There are no conflicts to declare.

Acknowledgements

This study was funded by the Austrian Science Fund (FWF) project number P 27689-N28

References

1 EBC, *European Biochar Certificate – Guidelines for a Sustainable Production of Biochar*, European Biochar Foundation (EBC), 2012, vol. 8, p. 2019.
2 J. Lehmann and S. Joseph, Biochar for environmental management: an introduction, in *Biochar for environmental management 2009*, Earthscan, 2009.
3 C. H. Chia, A. Downie and P. Munroe, Characteristics of biochar – physical and structural properties, in *Biochar for Environmental Management – Science and Technology 2009*, Earthscan Publications Ltd, 2009, 89–108, DOI: 10.4324/9780203762264.
4 J. Lehmann, A handful of carbon, *Nature*, 2007, **447**, 143–144.
5 N. Hagemann, *et al.*, Organic coating on biochar explains its nutrient retention and stimulation of soil fertility, *Nat. Commun.*, 2017, **8**, 1–11.
6 L. Beesley, *et al.*, A review of biochars' potential role in the remediation, revegetation and restoration of contaminated soils, *Environ. Pollut.*, 2011, **159**, 3269–3282.
7 J. Major, J. Lehmann, M. Rondon and C. Goodale, Fate of soil-applied black carbon: Downward migration, leaching and soil respiration, *Glob. Change Biol.*, 2010, **16**, 1366–1379.
8 K. A. Spokas, *et al.*, Physical disintegration of biochar: An overlooked process, *Environ. Sci. Technol. Lett.*, 2014, **1**, 326–332.
9 W. Yang, *et al.*, Effect of naphthalene on transport and retention of biochar colloids through saturated porous media, *Colloids Surf., A*, 2017, **530**, 146–154.
10 M. Chen, *et al.*, Transport and retention of biochar nanoparticles in a paddy soil under environmentally-relevant solution chemistry conditions, *Environ. Pollut.*, 2017, **230**, 540–549.
11 W. Zhang, *et al.*, Transport and retention of biochar particles in porous media: effect of pH, ionic strength, and particle size, *Ecohydrology*, 2010, **3**, 497–508.
12 D. Wang, W. Zhang, X. Hao and D. Zhou, Transport of biochar particles in saturated granular media: Effects of pyrolysis temperature and particle size, *Environ. Sci. Technol.*, 2013, **47**, 821–828.
13 B. Song, M. Chen, L. Zhao, H. Qiu and X. Cao, Physicochemical property and colloidal stability of micron- and nano-particle biochar derived from a variety of feedstock sources, *Sci. Total Environ.*, 2019, **661**, 685–695.
14 C. I. Czimczik and C. A. Masiello, Controls on black carbon storage in soils, *Global Biogeochem. Cycles*, 2007, **21**, 1–8.
15 G. Sigmund, C. Jiang, T. Hofmann and W. Chen, Environmental transformation of natural and engineered carbon nanoparticles and implications for the fate of organic contaminants, *Environ. Sci. Nano*, 2018, **5**, 2500–2518.
16 E. J. W. Verwey, Theory of the stability of lyophobic colloids, *J. Phys. Chem.*, 1947, **51**, 631–636.
17 B. Derjaguin and L. Landau, Theory of the stability of strongly charged lyophobic sols and of the adhesion of strongly charged particles in solutions of electrolytes, *Prog. Surf. Sci.*, 1993, **43**, 30–59.
18 S. Bhattacharjee, C. Ko and M. Elimelech, DLVO interaction between rough surfaces, *Langmuir*, 1998, **14**, 3365–3375.
19 F. Xu, *et al.*, Aggregation behavior of dissolved black carbon: Implications for vertical mass flux and fractionation in aquatic systems, *Environ. Sci. Technol.*, 2017, **51**, 13723–13732.
20 W. B. Hardy, A preliminary investion of the conditions which determine the stability of irreversible hydrosols, *J. Phys. Chem.*, 1900, 235–253, DOI: 10.1021/j150022a001.
21 H. Schulze, Schwefelarsen in wässriger Lösung, *J. Prakt. Chem.*, 1882, **25**, 431–452.
22 M. Gray, M. G. Johnson, M. I. Dragila and M. Kleber, Water uptake in biochars: The roles of porosity and hydrophobicity, *Biomass Bioenergy*, 2014, **61**, 196–205.
23 Z. Chen, B. Chen and C. T. Chiou, Fast and slow rates of naphthalene sorption to biochars produced at different temperatures, *Environ. Sci. Technol.*, 2012, **46**, 11104–11111.

24 W. Guo, Y. Ai, B. Men and S. Wang, Adsorption of phenanthrene and pyrene by biochar produced from the excess sludge: experimental studies and theoretical analysis, *Int. J. Environ. Sci. Technol.*, 2017, **14**, 1889–1896.
25 S. E. Hale, K. Hanley, J. Lehmann, A. R. Zimmerman and G. Cornelissen, Effects of Chemical, Biological, and Physical Aging As Well As Soil Addition on the Sorption of Pyrene to Activated Carbon and Biochar (vol 45, pg 10445, 2011), *Environ. Sci. Technol.*, 2012, **46**, 2479–2480.
26 M. Ahmad, *et al.*, Biochar as a sorbent for contaminant management in soil and water: A review, *Chemosphere*, 2014, **99**, 19–23.
27 G. Cornelissen, *et al.*, Extensive sorption of organic compounds to black carbon, coal, and kerogen in sediments and soils: Mechanisms and consequences for distribution, bioaccumulation, and biodegradation, *Environ. Sci. Technol.*, 2005, **39**, 6881–6895.
28 OECD, *Guideline 106 for the testing of chemicals- Adsorption – Desorption Using a Batch Equilibrium Method*, OECD Organisation for Economic Co-Operation and Development, 2000, DOI: 10.1787/9789264069602-en.
29 W. Yang, *et al.*, Colloidal stability and aggregation kinetics of biochar colloids: Effects of pyrolysis temperature, cation type, and humic acid concentrations, *Sci. Total Environ.*, 2019, **658**, 1306–1315.
30 Y. Wang, W. Zhang, J. Shang, C. Shen and S. D. Joseph, Chemical Aging Changed Aggregation Kinetics and Transport of Biochar Colloids, *Environ. Sci. Technol.*, 2019, **53**, 8136–8146.
31 F. Xu, *et al.*, Aggregation Behavior of Dissolved Black Carbon: Implications for Vertical Mass Flux and Fractionation in Aquatic Systems, *Environ. Sci. Technol.*, 2017, **51**, 13723–13732.
32 M. Kah, X. Zhang, M. T. O. Jonker and T. Hofmann, Measuring and modeling adsorption of PAHs to carbon nanotubes over a six order of magnitude wide concentration range, *Environ. Sci. Technol.*, 2011, **45**, 6011–6017.
33 M. Kah, G. Sigmund, P. L. Manga Chavez, L. Bielská and T. Hofmann, Sorption to soil, biochar and compost: is prediction to multicomponent mixtures possible based on single sorbent measurements?, *PeerJ*, 2018, **6**, e4996.
34 B. Song, M. Chen, L. Zhao, H. Qiu and X. Cao, Physicochemical property and colloidal stability of micron- and nano-particle biochar derived from a variety of feedstock sources, *Sci. Total Environ.*, 2019, **661**, 685–695.
35 X. Qu and D. Zhu, *Aggregation Behavior of Dissolved Black Carbon: Implications for Vertical Mass Flux and Fractionation in Aquatic Systems*, 2017, DOI: 10.1021/acs.est.7b04232.
36 B. Chen, D. Zhou and L. Zhu, Transitional Adsorption and Partition of Nonpolar and Polar Aromatic Contaminants by Biochars of Pine Needles with Different Pyrolytic Temperatures, *Environ. Sci. Technol.*, 2008, **42**, 5137–5143.
37 D. Zhu and J. J. Pignatello, Characterization of aromatic compound sorptive interactions with black carbon (charcoal) assisted by graphite as a model, *Environ. Sci. Technol.*, 2005, **39**, 2033–2041.
38 C. T. Chiou, J. Cheng, W. N. Hung, B. Chen and T. F. Lin, Resolution of adsorption and partition components of organic compounds on black carbons, *Environ. Sci. Technol.*, 2015, **49**, 9116–9123.
39 J. Wang, Z. Chen and B. Chen, Adsorption of Polycyclic Aromatic Hydrocarbons by Graphene and Graphene Oxide Nanosheets, *Environ. Sci. Technol.*, 2014, **48**, 4817–4825.
40 J. Wang, Z. Chen and B. Chen, Adsorption of polycyclic aromatic hydrocarbons by graphene and graphene oxide nanosheets, *Environ. Sci. Technol.*, 2014, **48**, 4817–4825.
41 X. Qu, Y. S. Hwang, P. J. J. Alvarez, D. Bouchard and Q. Li, UV irradiation and humic acid mediate aggregation of aqueous fullerene (nC 60) nanoparticles, *Environ. Sci. Technol.*, 2010, **44**, 7821–7826.
42 B. Smith, *et al.*, Influence of Surface Oxides on the Colloidal Stability of Multi-Walled Carbon Nanotubes: A Structure – Property Relationship, *Langmuir*, 2009, **25**, 9767–9776.
43 D. Quiñonero, *et al.*, Interplay between cation–π, anion–π and π–π interactions, *ChemPhysChem*, 2006, **7**, 2487–2491.
44 D. Kim, E. C. Lee, K. S. Kim and P. Tarakeshwar, Cation–π–anion interaction: A theoretical investigation of the role of induction energies, *J. Phys. Chem. A*, 2007, **111**, 7980–7986.

